Research Square

Preprints are preliminary reports that have not undergone peer review.
They should not be considered conclusive, used to inform clinical practice,
or referenced by the media as validated information.

Biomechanical Study of Bone Cement Reinforcement in Anterior Cervical Subtotal Discectomy and Fusion: A Finite Element Analysis

Zening Wang
Graduate School of Dalian Medical University
Anwu Xuan
Command General Hospital of the Chinese People's Liberation Army
Yanchun Xie
Command General Hospital of the Chinese People's Liberation Army
Yongcun Wei
University of Traditional Chinese Medicine
Yi Lian
Command General Hospital of the Chinese People's Liberation Army
Hongwen Gu
Command General Hospital of the Chinese People's Liberation Army
Hailong Yu
yuhailong118@aliyun.com

Command General Hospital of the Chinese People's Liberation Army

Research Article

Keywords: anterior cervical corpectomy and fusion, finite element analysis, Bone cement reinforcement, biomechanics

Posted Date: June 8th, 2026

DOI: https://doi.org/10.21203/rs.3.rs-9610962/v1

License: This work is licensed under a Creative Commons Attribution 4.0 International License.
Read Full License

Additional Declarations: No competing interests reported.

Biomechanical Study of Bone Cement Reinforcement in Anterior Cervical Subtotal Discectomy and Fusion: A Finite Element Analysis

Zening Wang[1,2†] ,Anwu Xuan [2†], Yanchun Xie[2], Yongcun Wei[3], Yi Lian[2],Hongwen Gu[2], Hailong Yu[2*]

(1. Graduate School of Dalian Medical University, Dalian, China; 2. Spinal Surgery Department of the Northern Theater Command General Hospital of the Chinese People's Liberation Army, Shenyang, China; 3. Graduate School of Liaoning University of Traditional Chinese Medicine, Shenyang, China)

【Abstract】

Cervical spondylosis is traditionally treated surgically by anterior cervical subtotal discectomy and fusion (ACCF). This study aims to investigate, via finite element analysis, the biomechanical effects of vertebral screw cement augmentation on adjacent endplates during anterior cervical subtotal discectomy and fusion (ACCF). This evaluates its efficacy in reducing the risk of titanium mesh subsidence and enhancing screw stability. Finite element models of the C4-C6 section were created using CT data from healthy subjects. Three cement-reinforced models and a traditional non-reinforced model made up the four surgical models. Different physiological activities were simulated at 74 N axial preload and 1 N·m pure torque. Screw stability (defined by the load-displacement ratio) and the maximal Von Mises stress at neighboring vertebral endplates were examined and contrasted. The results showed that despite improving screw stability, cement-augmented models decreased maximum stress at the C4 inferior endplate and C6 superior endplate. In comparison to the non-augmented group, the head-augmented model (M1) showed the most noticeable effects during hyperextension: stress at the C4 and C6 endplates dropped by 51.6% and 31.4%, respectively, while screw stability increased by an average of 50.1%. The results show that cement augmentation of the screw head region during ACCF surgery greatly improves screw fixation strength and most efficiently distributes load over adjacent vertebral endplates. This offers a useful biomechanical method for lowering the possibility of titanium mesh subsidence following surgery.

KEYWORDS:

anterior cervical corpectomy and fusion; finite element analysis; Bone cement reinforcement; biomechanics

1. Introduction

Cervical spondylotic myelopathy (CSM) refers to a gradually advancing neurological disorder that emerges as a result of degenerative alterations in the cervical spine, which subsequently cause compression of the spinal cord and adjacent anatomical structures [1]. Anterior cervical discectomy and fusion (ACDF) and anterior cervical corpectomy and fusion (ACCF) represent established surgical interventions commonly employed in the management of cervical spondylotic myelopathy [2]. Anterior cervical spine surgery can be accompanied by procedure-related complications, including injury to the superior laryngeal nerve and recurrent laryngeal nerve, postoperative cervical hematoma, spinal cord or nerve root damage, cerebrospinal fluid leakage, wound infection, and displacement of bone graft fragments. Additionally, complications associated with internal fixation

CONTACT Hailong YU ✉ yuhailong118@aliyun.com

†The first two authors contributed equally to this work.

devices are garnering growing concern in the clinical community [3-5]. Complications related to internal fixation devices encompass screw loosening, subsidence of cages and titanium mesh, among others. [6]. In elderly patients diagnosed with osteoporosis, the retention strength of screws is notably diminished in comparison to that observed in healthy adult individuals. Additionally, empirical studies have identified osteoporosis as a critical risk factor contributing to the migration of titanium mesh [7] [8]. Comprehensive experimental investigations have demonstrated that polymethyl methacrylate (PMMA) offers strong internal fixation at the interface between bone and screw. The injection of bone cement into the screw canal serves the dual purpose of altering the fixation interface and improving the stability of the screw [9] [10]. At present, research investigating the mechanical alterations at the titanium-cortical bone interface subsequent to anterior cervical vertebral screw reinforcement remains limited. In the present study, a proprietary finite element (FE) model of the cervical spine was utilized to simulate both conventional anterior cervical corpectomy and fusion (ACCF) procedures and ACCF procedures augmented with cemented vertebral screws. These models underwent in vitro biomechanical simulation testing to assess and compare the biomechanical performance of standard ACCF against cement-reinforced ACCF techniques. The evaluation focused on parameters including the maximum stress experienced at adjacent vertebral endplates and the stability of the implanted screws.

2. Materials and methodology

2.1. Subject for biomechanics simulation

A single healthy male volunteer, aged 23 years, with a height of 176 cm and a weight of 69 kg, was recruited for this study. The participant had no history of cervical spine disorders, and the presence of occipito-cervical deformities, tumors, infections, or fractures was excluded. Imaging was conducted using a 64-slice CT scanner at the CT Department of the Medical Imaging Centre, Northern Theatre Command General Hospital. A thin-slice spiral CT scan was performed with parameters set at 120 kV, 125 mA, and a slice thickness of 0.625 mm, covering the spinal segments from C2 to T2. The resulting CT data were exported and stored in DICOM format, comprising a total of 260 images. The procedure was approved by the Ethics Committee of the Northern Theatre Command General Hospital, People's Liberation Army and the patients provided written informed consent to participate in this study. Ethics Approval Number: EAPR Y (2025) No. 463

2.2. Establishment of a standard C4-6 finite element model

The scanned CT data were imported into Mimics 21.0 (Materialise, Belgium) for segmentation of each vertebral body. Utilizing the human skeletal threshold, a mask representing the normal cervical spine from C4 to C6 was generated and subsequently saved in STL format. The STL file was then imported into Geomagic Wrap 2021 (Geomagic, USA) for processes including re-meshing, patching, smoothing, denoising, cutting, surface refinement, and reconstruction, thereby approximating the bony architecture of the cervical spine. This methodology was applied to develop models of both cortical and cancellous bone, which were exported in STP format. The cancellous and cortical bone models were then imported into SolidWorks (Dassault Systèmes, USA) for reassembly. In accordance with existing literature and anatomical data, the annulus fibrosus and nucleus pulposus were delineated using a proportional division of 60% to 40%, respectively [11] [12]. Simultaneously establish articular cartilage. As shown in Figure 1.

2.3. Establishment FE models of ACCF

Using SolidWorks software, an anterior cervical titanium plate and corresponding screws were designed. The established C4-6 model simulated the resection of the anterior longitudinal ligament,

posterior longitudinal ligament, and the intervertebral disc between C5 and C6, followed by a subtotal resection of the C5 vertebral body while preserving the bilateral Luschka joint. This reconstruction was achieved through the application of a titanium plate and vertebral body screws (VBS). The VBS were oriented parallel to the inferior endplate of C4 and the superior endplate of C6, with dimensions of 14 mm in length and 4 mm in diameter. This configuration was designated as model M0. For the bone cement augmentation groups, prior to the insertion of the VBS, 0.3 to 0.5 ml of bone cement was injected to a predetermined depth within each screw tract. Building upon the M0 model, three variants were developed based on the depth of cement injection: (1) M1, with bone cement injected into the screw head segment; (2) M2, with cement injected into the middle segment of the screw; and (3) M3, with cement injected into the tail segment of the screw. The constructed anterior cervical corpectomy and fusion (ACCF) models are illustrated in Figure 2.

2.4. Establishment of a Screw Stability Model

Based on the previously described model, a single C6 vertebral segment consisting of both cortical and cancellous bone was chosen. Cervical screws and bone cement were then implanted following the standardized ACCF model protocol. The grouping and nomenclature were maintained in accordance with prior conventions. The completed model for evaluating screw stability is illustrated in Figure 3.

2.5. Finite element analysis

The complete model was imported into ANSYS 23R2 software (ANSYS, Inc., USA), with material properties assigned according to parameters obtained from previous studies [12-15]. Specific material assignments are detailed in Table 1. The imported C4-6 model was meshed using tetrahedral elements for cortical bone, cancellous bone, screws, and titanium plates. Element sizes were set to 1 mm for cortical and cancellous bone, and 0.5 mm for screws and titanium plates. The annulus fibrosus, nucleus pulposus, and articular cartilage were modelled using hexahedral elements with a size of 0.5 mm. The cervical spine model established in this study comprised 745,528 nodes and 448,825 elements

1. 1. In the validation process of the comprehensive finite element model of the cervical spine, the inferior endplate of the C6 vertebra was constrained to eliminate all degrees of freedom. An axial load of 74 N was applied to the superior endplate of the C4 vertebra to represent the weight of the head, accompanied by a torque of 1 N·m. Subsequent to the application of these loads, the model was subjected to testing across seven distinct motions: axial positioning, flexion, extension, left and right lateral flexion, as well as left and right rotation.
2. The internal fixation model was subjected to a pure moment load of 1 N·m in conjunction with a preload of 74 N. Experimental evaluations were performed under seven distinct loading conditions applied to the superior surface of the C4 vertebra across four anterior cervical corpectomy and fusion (ACCF) finite element models.
3. To validate the stability of the screw, we established a friction relationship between the screw and the cortical bone, cancellous bone, and bone cement, with a friction coefficient of 0.1. The upper and lower endplates of the C6 vertebral body were fixed, restricting its degrees of freedom in all directions. Displacements of 0.1 mm were applied to the screw tail in the four directions: up, down, left, and right.

This study primarily focused on measuring: (1) The range of motion (ROM) of the C4-6 model to evaluate its validity; (2) The maximum Von Mises stress at the inferior endplate of C4 and the superior endplate of C6 across the four models, whilst comparing the endplate Von Mises stress

under different scenarios between reinforced and non-reinforced screw fixation techniques; (3) The magnitude of the load-displacement ratio for the four screw insertion methods, to assess screw stability.

3. Result

3.1. Validity of the Complete C4-6 Finite Element Model

To assess the validity of the model, the segmental range of motion (ROM) was quantified for each type of movement, and the resulting data were compared with findings reported in prior biomechanical experimental studies. When subjected to a pure moment of 1 Nm, the ROM values at the C4-5 (Figure 4A) and C5-6(Figure 4B) segments across six loading conditions exhibited minimal deviation from the in vitro mechanical experiments conducted by Panjabi et al. and Liu et al. [16 17]. As illustrated in Figure 4, the C4-6 model utilized in this study is deemed valid for subsequent analysis.

3.2. Von Mises stress on the surface of adjacent vertebrae

Figures 5 present the maximum Von Mises stresses observed at the inferior endplate of C4 (Figure 5A)and the superior endplate of C6 (Figure 5B) under flexion, axial rotation, and lateral bending loads across four fixation models. The influence of different bone cement reinforcement techniques on the Von Mises stresses at adjacent endplates varies notably. Among all anterior cervical corpectomy and fusion (ACCF) models, the M0 model exhibited the highest Von Mises stress at the terminal plates, followed sequentially by the M3 and M2 models, with the M1 model demonstrating the lowest stress levels. Stress contour maps for the C4 inferior and C6 superior terminal plates are illustrated in Figures 7 and 8, respectively. Analysis of stress distribution reveals that peak stresses are primarily localized in the mid-to-posterior regions of the terminal plates. Under seven distinct loading conditions, the peak stress values at the C4 endplate ranged from 14.707 MPa to 30.362 MPa, whereas those at the C6 endplate varied between 21.167 MPa and 30.843 MPa. The maximum Von Mises stresses at the endplates were recorded during extension. Notably, the M1 model demonstrated the most significant reduction in Von Mises stress at the C4 and C6 endplates during posterior extension, with decreases of 51.6% and 31.4%, respectively, relative to the M0 model. These reductions surpassed those observed in the M2 model (3.7% and 1.81%) and the M3 model (3.0% and 2.94%).

3.3. VBS Screw Stability

Across all directions of movement, the stability—measured by the load-displacement ratio—of screws reinforced with bone cement demonstrated a marked enhancement compared to non-reinforced screws, surpassing the unreinforced group's value of 2033.975 N/mm (refer to Figure 6). The most pronounced increase in stability was observed in the Group A reinforced models, which exhibited an average improvement of 50.1% relative to the unreinforced group, with a mean load-displacement ratio of 3053.7 N/mm. This was followed by Group B models, with a load-displacement ratio of 2464.4 N/mm, and Group C models, at 2254.375 N/mm, corresponding to stability enhancements of 21.2% and 10.9%, respectively, compared to the unreinforced screws.

4. Discussion

Anterior cervical corpectomy and fusion (ACCF) is one of the classic surgical procedures for treating cervical spondylosis. It offers advantages such as an unobstructed surgical field and thorough decompression, and is widely employed in clinical practice[18]. Following a subtotal vertebral resection, an implant must be inserted to maintain cervical spinal stability. The implant can utilise various bone graft materials to fill the postoperative vertebral void and preserve vertebral

height. Autologous iliac crest bone grafting was frequently employed in the early days for fusion, yet the donor site is also prone to various complications, such as haemorrhage, infection, haematoma, and donor site pain [19 20]. Titanium mesh was first applied in spinal surgery in 1986 [21], It not only offers structural reinforcement for the anterior column but also obviates the necessity for supplementary autogenous bone harvesting, thereby preventing donor site complications and enhancing the osseointegration rate [22 23]. However, the incidence of titanium mesh migration is relatively high. Since the 21st century, the structure of titanium mesh has undergone continuous refinement through the application of new technologies, resulting in a reduction in the incidence of mesh migration compared to previous generations [24]. Studies indicate that the rate of titanium mesh migration following ACCF procedures ranges from 21.3% to 79.7% [25 26], Van Jonbergen et al. proposed defining postoperative mesh descent of ≥3mm as mesh descent,[27] Previous studies have indicated that risk factors for titanium mesh migration include advanced age, osteoporosis, and long-segment subtotal vertebral resection [28 29], Osteoporosis is considered to significantly increase the risk of titanium mesh migration following spinal surgery [7 8], Concurrently, osteoporosis also increases the risk of screw loosening and dislodgement [30], In recent years, extensive research has been conducted on the use of pedicle screw fixation techniques for the treatment and repair of thoracolumbar injuries, and these methods have gained widespread clinical application [31 32].Currently, PMMA augmentation techniques represent a common method for reinforcing or repairing vertebral bodies or pedicle screws. When utilising PMMA to augment vertebral screws, the material diffuses within the vertebra along the trabeculae, enlarging the fixation interface between the bone cement and bone. This facilitates a more intimate union between the two components, thereby enhancing the holding strength at the screw-to-bone interface [10]. However, research on the use of PMMA for screw-track reinforcement in cervical internal fixation systems remains limited.

Finite element analysis is a computational approach that utilizes mathematical methods to model and simulate physical systems encountered in real-world scenarios. In 1974, Belytschko and colleagues were among the first to apply three-dimensional finite element analysis specifically within the context of spinal surgery [33], With the continuous enhancement of computational capabilities and the progressive refinement of finite element analysis (FEA) software, FEA technology has attained a high degree of sophistication. In comparison to in vitro experiments and clinical trials, finite element analysis presents distinct advantages, including reproducibility, cost efficiency, and improved safety. The establishment of a robust research model is critical to ensuring the reliability of finite element calculation outcomes. When the results derived from the model developed in this study are compared with range of motion (ROM) data obtained from in vitro experiments, such as those conducted by Panjiabi et al., the deviations observed remain within an acceptable margin. Moreover, the model demonstrates favorable biomechanical properties. This study also systematically classified the models and conducted surgical simulations on validated models to develop four distinct surgical paradigms. The analysis incorporated simulations of osteoporotic bone quality, with groups differentiated according to various positions of bone cement screw-channel reinforcement. The novelty of this research lies in its investigation of vertebral augmentation during cervical anterior cervical corpectomy and fusion (ACCF) surgery, specifically examining alterations in Von Mises stress on the superior and inferior vertebral endplates postoperatively, as well as the stability of vertebral screws following augmentation. Additionally,

the study provides a comparative analysis of the effects of vertebral cement augmentation at different anatomical locations.

Concerning alterations in endplate Von Mises stress, the current investigation demonstrates that subsequent to anterior cervical corpectomy and fusion (ACCF) surgery, the peak endplate Von Mises stress localizes predominantly within the mid-to-posterior region of the vertebral body. Notably, during extension movements, the escalation of Von Mises stress on the vertebral surface relative to the axial position is most significant. This phenomenon can be attributed to the stabilizing effect of the titanium plate on the anterior vertebral region, whereby the anterior vertebral pressure is partially borne by the titanium plate, while the posterior Von Mises stress is chiefly transmitted through the titanium mesh. In models subjected to vertebral augmentation, the M1 group demonstrated a substantial decrease in Von Mises stress during axial loading, flexion, and extension compared to Groups B and C. This reduction is likely due to the strategic placement of bone cement within the mid-to-posterior vertebral body in Group A models, coinciding with the region of concentrated endplate Von Mises stress following mesh insertion. As a result, a portion of the endplate stress in Group A is effectively shared by the intravertebral bone cement. Conversely, during lateral flexion and rotational movements, stress predominantly accumulates on both lateral aspects of the titanium mesh-endplate interface. Consequently, the diminution of endplate Von Mises stress during these motions is less pronounced. Importantly, the maximal stress observed at the titanium mesh-endplate interface constitutes a critical metric indicative of the potential risk for mesh subsidence [34]. The application of bone cement reinforcement facilitates the effective distribution of these stresses. Additionally, augmenting the strength of the screw heads can substantially improve vertebral stability and mitigate the risk of titanium mesh subsidence.

The analysis of screw stability indicated that all screws showed improved stability after vertebral augmentation, with the M1 group exhibiting the greatest enhancement. This phenomenon can be explained by the following mechanism: when lateral displacement forces are applied to the screw shaft, the cortical bone functions as a fulcrum, leading to relative sliding between the screw head and the cancellous bone. The reinforcement provided by bone cement increases resistance to this relative sliding, thereby augmenting screw stability post-reinforcement. Notably, the M1 group demonstrated the largest distance between the screw head and the cortical bone at the insertion site, which corresponds to the most significant improvement in stability.

Furthermore, the limitations of the present study must be acknowledged. First, the cervical spine models were generated from volunteers exhibiting normal, non-pathological conditions, which may result in minor biomechanical discrepancies when compared to patients suffering from pathological cervical spondylotic myelopathy who require anterior cervical surgery. Second, the analysis was confined to the immediate postoperative alterations in Von Mises stress at the superior and inferior endplates, as well as screw stability, without accounting for the long-term pathological progression in patients. Nonetheless, the principal findings of this investigation are based on comparative analyses across different surgical approach models. Lastly, the study did not include the modeling of cervical paravertebral musculature, focusing exclusively on critical ligamentous structures; as a result, the model may slightly deviate from true anatomical conditions. These limitations are consistent across all models and are unlikely to significantly affect the comparative results.

5. Conclusion

In summary, this study conducted a comparative analysis of the mechanical behavior of

endplates and screws across various anterior cervical fusion models. The results demonstrate that bone cement augmentation consistently decreases the maximum Von Mises stress on the endplates while improving screw stability. Notably, the application of bone cement to augment the screw head within the vertebral canal during anterior cervical vertebral screw placement effectively reduces Von Mises stress on adjacent vertebral surfaces under axial loading, flexion, and extension movements. This reduction in stress contributes to the mitigation of titanium mesh subsidence risk. The findings of this research provide novel insights and methodological approaches aimed at preventing titanium mesh subsidence following anterior cervical fusion surgery in clinical settings.

Disclosure statement

No potential conflict of interest was reported by the authors.

Funding

The authors declare that this research did not receive anyspecific grant from funding agencies in the public, commercial, or not-for-profit sectors.

Author contributions statement

Zening Wang and Anwu Xuan contributed equally to this work, Zening Wang was responsible for Conceptualization, Data curation, Formal analysis, Methodology, Software, Validation, Visualization, Writing – original draft. Anwu Xuan contributed to Project administration, Formal analysis, Supervision, Validation, Visualization, Writing – review & editing

Yanchun Xie was responsible for Resources.

Yongcun wei contributed to Visualization.

Yi Lian contributed to Investigation.

Hongwen Gu contributed to Project administration.

Hailong Yu: Conceptualization, Project administration, Supervision, Writing – Review & Editing.

All authors have read and agreed to the published version of the manuscript.

References

1. Bakhsheshian J, Mehta VA, Liu JC. Current Diagnosis and Management of Cervical Spondylotic Myelopathy. *Global Spine J* 2017;7(6):572-86. doi: 10.1177/2192568217699208 [published Online First: 2017/09/13]
2. Wen Z, Lu T, Wang Y, et al. Anterior Cervical Corpectomy and Fusion and Anterior Cervical Discectomy and Fusion Using Titanium Mesh Cages for Treatment of Degenerative Cervical Pathologies: A Literature Review. *Med Sci Monit* 2018;24:6398-404. doi: 10.12659/msm.910269 [published Online First: 2018/09/13]
3. Fountas KN, Kapsalaki EZ, Nikolakakos LG, et al. Anterior cervical discectomy and fusion associated complications. *Spine (Phila Pa 1976)* 2007;32(21):2310-7. doi: 10.1097/BRS.0b013e318154c57e [published Online First: 2007/10/02]
4. Rao RD, Gourab K, David KS. Operative treatment of cervical spondylotic myelopathy. *J Bone Joint Surg Am* 2006;88(7):1619-40. doi: 10.2106/jbjs.F.00014 [published Online First: 2006/07/05]
5. Sagi HC, Beutler W, Carroll E, et al. Airway complications associated with surgery on the anterior cervical spine. *Spine (Phila Pa 1976)* 2002;27(9):949-53. doi: 10.1097/00007632-200205010-00013 [published Online First: 2002/04/30]
6. Sasso RC, Ruggiero RA, Jr., Reilly TM, et al. Early reconstruction failures after multilevel cervical corpectomy. *Spine (Phila Pa 1976)* 2003;28(2):140-2. doi: 10.1097/00007632-200301150-00009 [published Online First: 2003/01/25]
7. Abudouaini H, Wu T, Liu H, et al. The predictive value of Hounsfield units for titanium mesh cage subsidence after anterior cervical corpectomy and fusion. *Front Surg* 2022;9:1012364. doi: 10.3389/fsurg.2022.1012364 [published Online First: 2023/01/24]
8. Wang J, Gao C, Zang F, et al. Predictive value of vertebral Hounsfiled Unit for titanium mesh cage subsidence following ACCF surgery. *Clin Neurol Neurosurg* 2024;236:108047. doi: 10.1016/j.clineuro.2023.108047 [published Online First: 2023/11/21]
9. Choma TJ, Pfeiffer FM, Swope RW, et al. Pedicle screw design and cement augmentation in osteoporotic vertebrae: effects of fenestrations and cement viscosity on fixation and extraction. *Spine (Phila Pa 1976)* 2012;37(26):E1628-32. doi: 10.1097/BRS.0b013e3182740e56 [published Online First: 2012/09/22]
10. Hoppe S, Loosli Y, Baumgartner D, et al. Influence of screw augmentation in posterior dynamic and rigid stabilization systems in osteoporotic lumbar vertebrae: a biomechanical cadaveric study. *Spine (Phila Pa 1976)* 2014;39(6):E384-9. doi: 10.1097/brs.0000000000000198 [published Online First: 2014/01/05]
11. Denozière G, Ku DN. Biomechanical comparison between fusion of two vertebrae and implantation of an artificial intervertebral disc. *J Biomech* 2006;39(4):766-75. doi: 10.1016/j.jbiomech.2004.07.039 [published Online First: 2006/01/28]
12. Wu TK, Meng Y, Liu H, et al. Biomechanical effects on the intermediate segment of noncontiguous hybrid surgery with cervical disc arthroplasty and anterior cervical discectomy and fusion: a finite element analysis. *Spine J* 2019;19(7):1254-63. doi: 10.1016/j.spinee.2019.02.004 [published Online First: 2019/02/12]
13. Zhang QH, Teo EC, Ng HW, et al. Finite element analysis of moment-rotation relationships for human cervical spine. *J Biomech* 2006;39(1):189-93. doi: 10.1016/j.jbiomech.2004.10.029 [published Online First: 2005/11/08]

14. Li Y, Lewis G. Influence of surgical treatment for disc degeneration disease at C5-C6 on changes in some biomechanical parameters of the cervical spine. *Med Eng Phys* 2010;32(6):595-603. doi: 10.1016/j.medengphy.2010.02.009 [published Online First: 2010/03/10]
15. Nobakhti S, Shefelbine SJ. On the Relation of Bone Mineral Density and the Elastic Modulus in Healthy and Pathologic Bone. *Curr Osteoporos Rep* 2018;16(4):404-10. doi: 10.1007/s11914-018-0449-5 [published Online First: 2018/06/06]
16. Liu Q, Guo Q, Yang J, et al. Subaxial Cervical Intradiscal Pressure and Segmental Kinematics Following Atlantoaxial Fixation in Different Angles. *World Neurosurg* 2016;87:521-8. doi: 10.1016/j.wneu.2015.09.025 [published Online First: 2015/09/27]
17. Panjabi MM, Crisco JJ, Vasavada A, et al. Mechanical properties of the human cervical spine as shown by three-dimensional load-displacement curves. *Spine (Phila Pa 1976)* 2001;26(24):2692-700. doi: 10.1097/00007632-200112150-00012 [published Online First: 2001/12/12]
18. Jiang SD, Jiang LS, Dai LY. Anterior cervical discectomy and fusion versus anterior cervical corpectomy and fusion for multilevel cervical spondylosis: a systematic review. *Arch Orthop Trauma Surg* 2012;132(2):155-61. doi: 10.1007/s00402-011-1402-6 [published Online First: 2011/10/05]
19. Malloy KM, Hilibrand AS. Autograft versus allograft in degenerative cervical disease. *Clin Orthop Relat Res* 2002(394):27-38. doi: 10.1097/00003086-200201000-00004 [published Online First: 2002/01/25]
20. Silber JS, Anderson DG, Daffner SD, et al. Donor site morbidity after anterior iliac crest bone harvest for single-level anterior cervical discectomy and fusion. *Spine (Phila Pa 1976)* 2003;28(2):134-9. doi: 10.1097/00007632-200301150-00008 [published Online First: 2003/01/25]
21. Riew KD, Rhee JM. The use of titanium mesh cages in the cervical spine. *Clin Orthop Relat Res* 2002(394):47-54. doi: 10.1097/00003086-200201000-00006 [published Online First: 2002/01/25]
22. Chuang HC, Cho DY, Chang CS, et al. Efficacy and safety of the use of titanium mesh cages and anterior cervical plates for interbody fusion after anterior cervical corpectomy. *Surg Neurol* 2006;65(5):464-71; discussion 71. doi: 10.1016/j.surneu.2005.12.021 [published Online First: 2006/04/25]
23. Nakase H, Park YS, Kimura H, et al. Complications and long-term follow-up results in titanium mesh cage reconstruction after cervical corpectomy. *J Spinal Disord Tech* 2006;19(5):353-7. doi: 10.1097/01.bsd.0000210113.09521.aa [published Online First: 2006/07/11]
24. Fiani B, Newhouse A, Cathel A, et al. Implications of 3-Dimensional Printed Spinal Implants on the Outcomes in Spine Surgery. *J Korean Neurosurg Soc* 2021;64(4):495-504. doi: 10.3340/jkns.2020.0272 [published Online First: 2021/06/19]
25. Chen Y, Chen D, Guo Y, et al. Subsidence of titanium mesh cage: a study based on 300 cases. *J Spinal Disord Tech* 2008;21(7):489-92. doi: 10.1097/BSD.0b013e318158de22 [published Online First: 2008/10/07]
26. Hirai T, Yoshii T, Egawa S, et al. Increased Height of Fused Segments Contributes to Early-Phase Strut Subsidence after Anterior Cervical Corpectomy with Fusion for Multilevel Ossification of the Posterior Longitudinal Ligament. *Spine Surg Relat Res* 2020;4(4):294-99. doi: 10.22603/ssrr.2019-0102 [published Online First: 2020/11/17]

27. van Jonbergen HP, Spruit M, Anderson PG, et al. Anterior cervical interbody fusion with a titanium box cage: early radiological assessment of fusion and subsidence. *Spine J* 2005;5(6):645-9; discussion 49. doi: 10.1016/j.spinee.2005.07.007 [published Online First: 2005/11/18]
28. Pinter ZW, Reed R, Townsley SE, et al. Titanium Cervical Cage Subsidence: Postoperative Computed Tomography Analysis Defining Incidence and Associated Risk Factors. *Global Spine J* 2023;13(7):1703-15. doi: 10.1177/21925682211046897 [published Online First: 2021/09/25]
29. Jang JW, Lee JK, Lee JH, et al. Effect of posterior subsidence on cervical alignment after anterior cervical corpectomy and reconstruction using titanium mesh cages in degenerative cervical disease. *J Clin Neurosci* 2014;21(10):1779-85. doi: 10.1016/j.jocn.2014.02.016 [published Online First: 2014/06/25]
30. Frankel BM, D'Agostino S, Wang C. A biomechanical cadaveric analysis of polymethylmethacrylate-augmented pedicle screw fixation. *J Neurosurg Spine* 2007;7(1):47-53. doi: 10.3171/spi-07/07/047 [published Online First: 2007/07/19]
31. Kiner DW, Wybo CD, Sterba W, et al. Biomechanical analysis of different techniques in revision spinal instrumentation: larger diameter screws versus cement augmentation. *Spine (Phila Pa 1976)* 2008;33(24):2618-22. doi: 10.1097/BRS.0b013e3181882cac [published Online First: 2008/11/18]
32. Liu D, Zhang Y, Zhang B, et al. Comparison of expansive pedicle screw and polymethylmethacrylate-augmented pedicle screw in osteoporotic sheep lumbar vertebrae: biomechanical and interfacial evaluations. *PLoS One* 2013;8(9):e74827. doi: 10.1371/journal.pone.0074827 [published Online First: 2013/10/03]
33. Belytschko T, Kulak RF, Schultz AB, et al. Finite element stress analysis of an intervertebral disc. *J Biomech* 1974;7(3):277-85. doi: 10.1016/0021-9290(74)90019-0 [published Online First: 1974/05/01]
34. Zhou E, Huang H, Zhao Y, et al. The effects of titanium mesh cage size on the biomechanical responses of cervical spine after anterior cervical corpectomy and fusion: A finite element study. *Clin Biomech (Bristol)* 2022;91:105547. doi: 10.1016/j.clinbiomech.2021.105547 [published Online First: 2021/12/20]

Table 1. Material properties of spine tissues used in the finite element model.

Property	Modulus (MPa)	Ratio	Cross-sectional area(mm2)	Element type
Cortical bone	12000	0.3	-	Tetrahedral element
Cortical bone（Osteoporosis）	8040	0.3	-	Tetrahedral element
Cancellous bone	450	0.2	-	Tetrahedral element
Cancellous bone（Osteoporosis）	50	0.2	-	Tetrahedral element
Annulus fibrosus	4.2	0.45	-	Hexahedral element
Bone cement	4000	0.33	-	Tetrahedral element
Nucleus pulposus	1	0.49	-	Hexahedral element
Anterior longitudinal ligament	10	0.3	6	Cable element
Posterior longitudinal ligament	10	0.3	5	Cable element
Ligamentum flavum	1.5	0.3	5	Cable element
Interspinous Ligament	1.5	0.3	10	Cable element
Supraspinous ligament	1.5	0.3	5	Cable element
Intertransverse ligament	1.5	0.3	5	Cable element
Capsular ligament	10	0.3	46	Cable element
Titanium alloy material	110000	0.3	-	Tetrahedral element

Figure 1. Finite element model of intact C4-C6 levels.

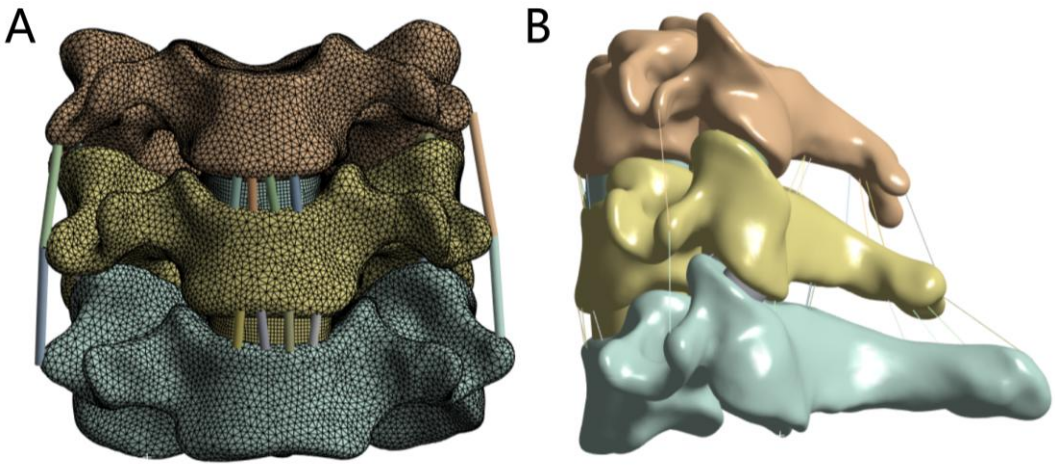


Figure 2. Lateral and AP view of four ACCF FE models. M0 means the ACCF model with plain titanium plate screws. M1 means the ACCF model with bone cement reinforcement in the screw head section. M2 means the ACCF model with bone cement reinforcement in the middle section of the screw. M3 means the ACCF model with bone cement reinforcement in the tail section of the screw.

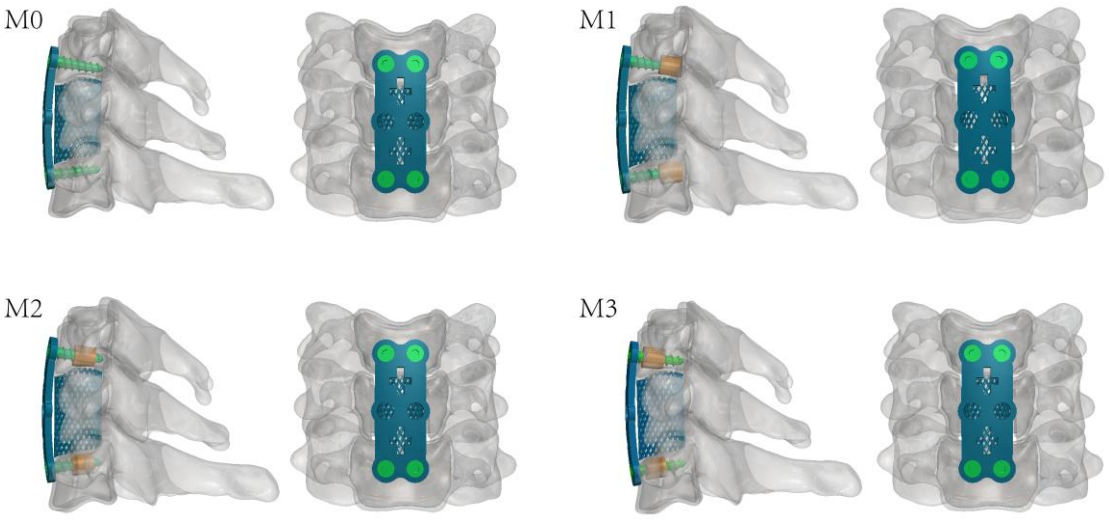


Figure 3. The lateral and overhead views of the C6 screw stability test model, where M0 means no bone cement reinforcement, M1 means bone cement reinforcement at the screw head section, M2 means bone cement reinforcement at the screw middle section, and M3 means bone cement reinforcement at the screw tail section.

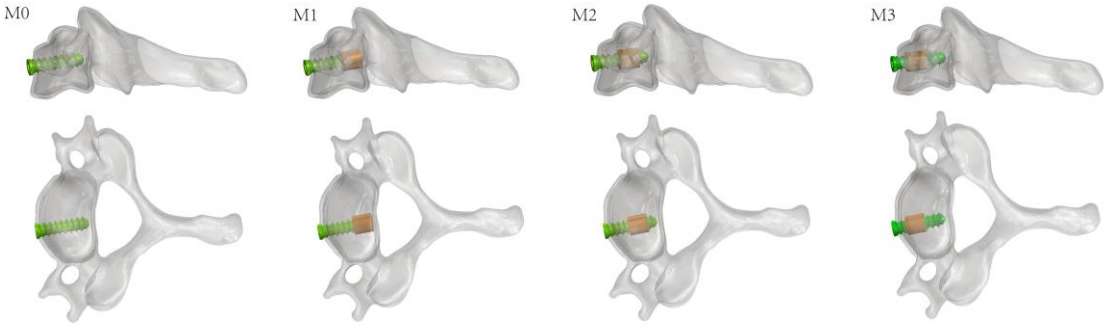
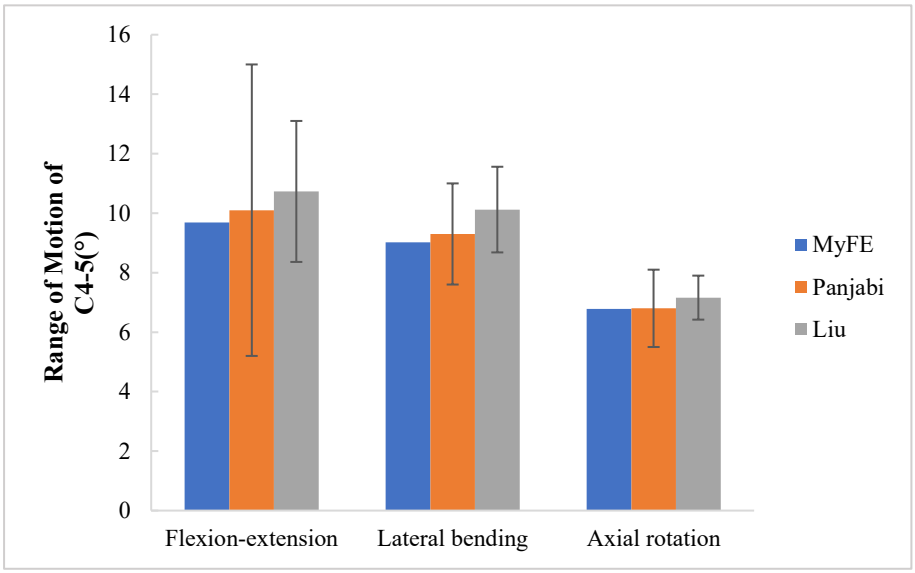


Figure 4. Validation of the present intact C4-6 FE model with in vitro cadaveric study by Panjabi et al. and Liu et al. A: Comparisonof ROM at level C4-C5. B: Comparison of ROM at level C5-C6.

A



B

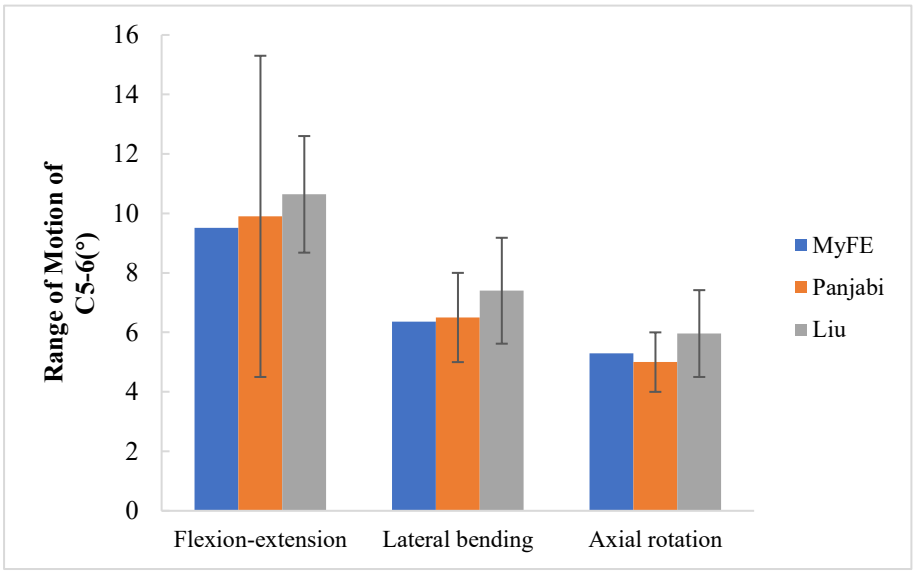
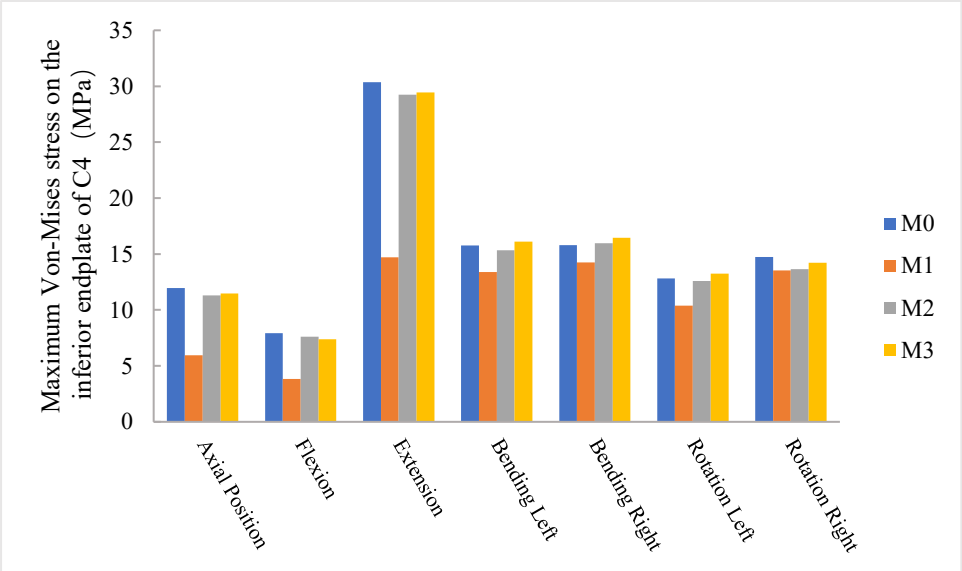


Figure 5. The maximum von Mises stress of the adjacent end plates of the titanium meshduring all motions A: Maximum Von-Mises stress on the inferior endplate of C4, B: Maximum Von-Mises stress on the superior endplate of C6

A



B

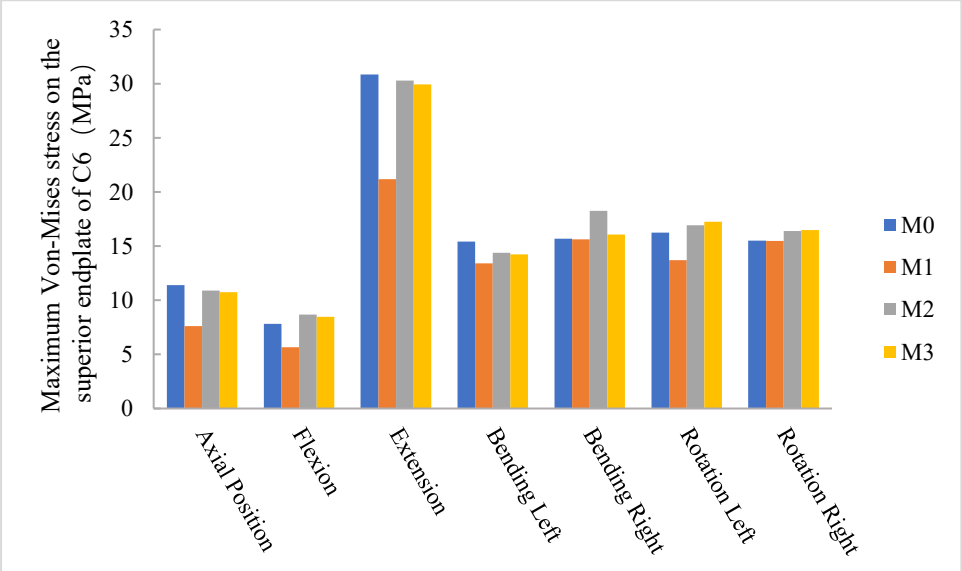


Figure 6. Screw load-displacement ratio for four models

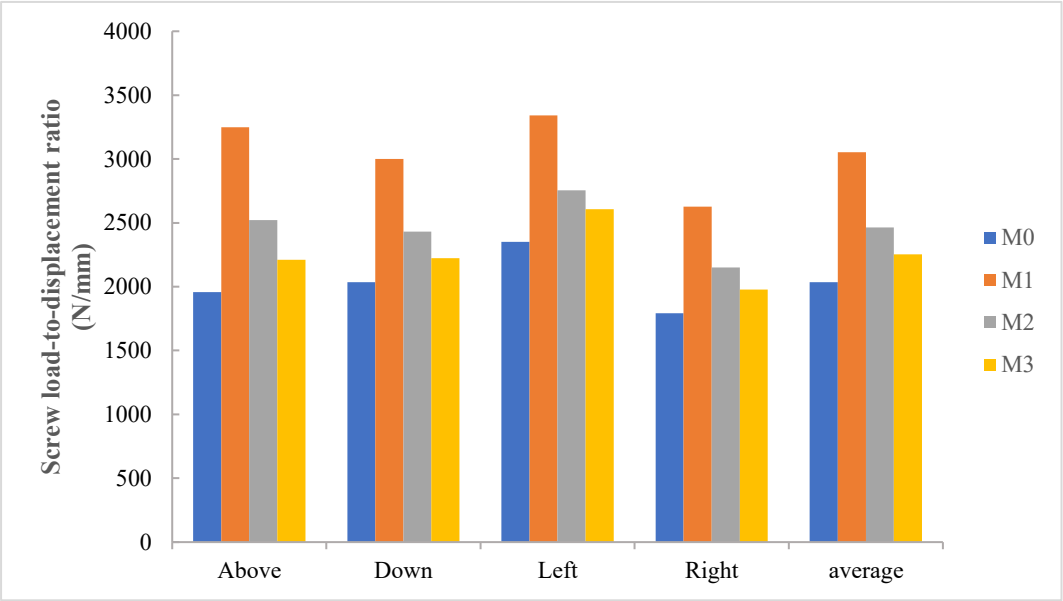


Figure 7. Stress contour plots of the endplate under four C4 models, from top to bottom: axial position, flexion, extension, bending left, bending right, rotation left, rotation right.

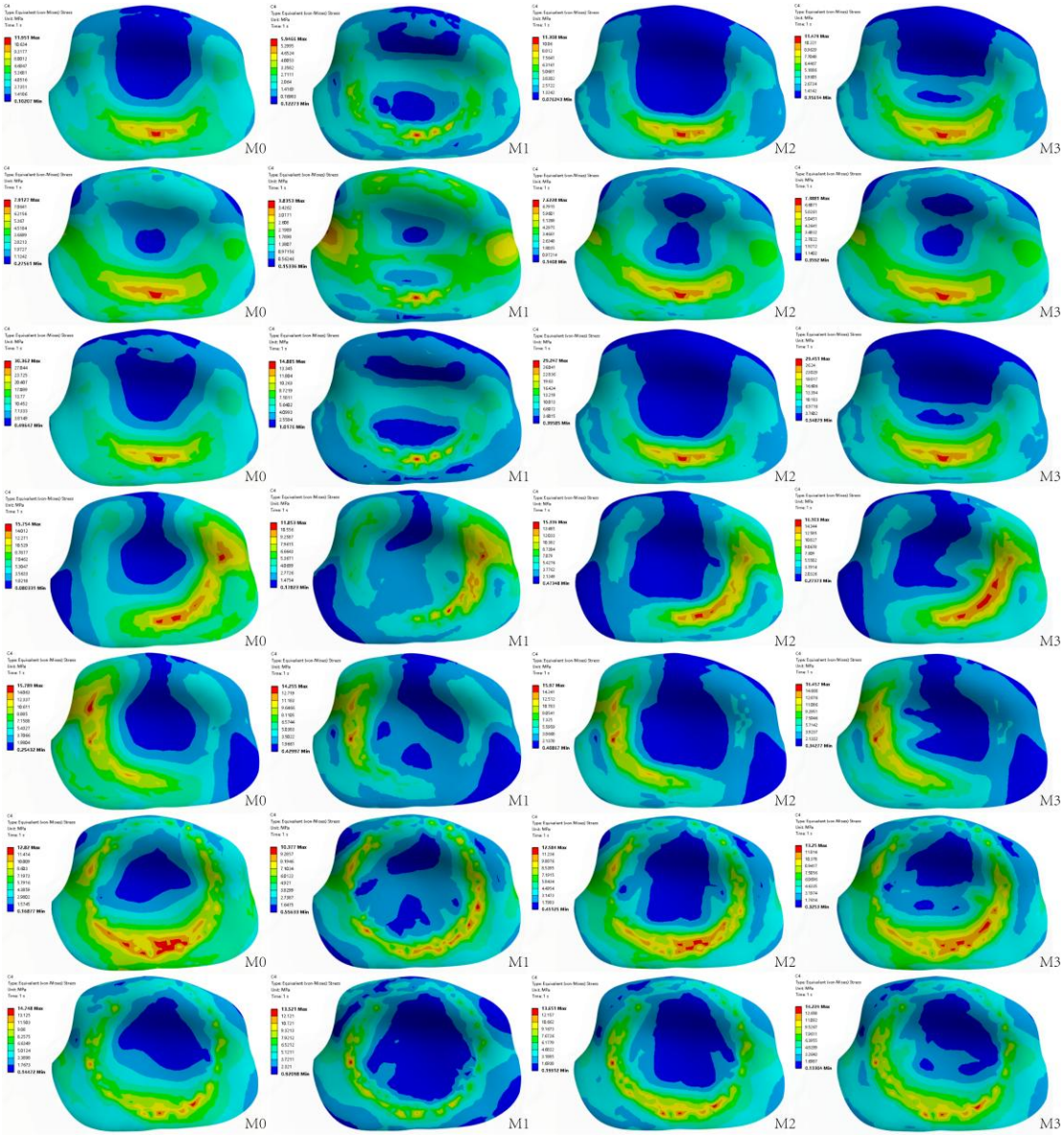


Figure 8. Stress contour plots for the terminal plate of the C6 vertebra across four model sets, from top to bottom: axial position, flexion, extension, bending left, bending right, rotation left, rotation right.

